Cooperative Estimation of Maps of Physical and Virtual Radio Transmitters

Markus Ulmschneider, Christian Gentner and Armin Dammann

German Aerospace Center (DLR), Institute of Communications and Navigation

ABSTRACT

In multipath assisted positioning, the spatial information contained in multipath components (MPCs) is exploited, as MPCs are regarded as line-of-sight signals from virtual transmitters. The positions of physical and virtual transmitters can be estimated jointly with the receiver position with simultaneous localization and mapping (SLAM). In our multipath assisted positioning approach called Channel-SLAM, the estimates from a channel estimator are used in a Rao-Blackwellized particle filter which implements SLAM. While the original Channel-SLAM algorithm is a single-user positioning system, we present a comprehensive framework for cooperative Channel-SLAM within this paper. Users cooperate by exchanging maps of estimated transmitter locations. With prior information about the locations of physical and virtual transmitters, the positioning performance of the users increases significantly. The more users contribute to such a transmitter map, the more increases the positioning performance. With simulations in an indoor scenario, we show that the positioning performance is bounded for cooperative Channel-SLAM in the long run.

BIOGRAPHIES

Markus Ulmschneider received his Master's degree in 2014 from the University of Ulm, and his PhD from the Hamburg University of Technology in 2021. Since 2014, he has been working at the Institute of Communications and Navigation of the German Aerospace Center (DLR), focusing on multipath assisted positioning.

Christian Gentner received his M.Sc. and Dr.-Ing. (Ph.D.) degrees in electrical Engineering in 2009 and 2018, respectively, from the University of Ulm. Since 2009, he is working at the Institute of Communications and Navigation of the German Aerospace Center (DLR). His current research focuses on multipath assisted and indoor positioning.

Armin Dammann received his Diploma (Dipl.-Ing.) and PhD (Dr.-Ing.) from the University of Ulm in 1997 and 2005 respectively. In 1997 he joined the Institute of Communications and Navigation of the German Aerospace Center (DLR). Since 2005 he is head of the Mobile Radio Transmission research group of the institute.

I. INTRODUCTION

Multipath propagation has been considered harmful for localization techniques that are based on the estimation of parameters of wireless radio signals such as delay or received signal strength indicator (RSSI). In contrast, multipath assisted positioning is a concept that exploits the spatial information contained in multipath components (MPCs) for localization of a receiver. The idea is to treat MPCs as signals from virtual transmitters in a line-of-sight (LoS) condition. While the locations of both the physical and such virtual transmitters are typically unknown, they can be estimated jointly with a receiver position with simultaneous localization and mapping (SLAM) [1, 2].

Various such SLAM based algorithms and analyses have been presented in the literature. Since the bandwidth of the transmit signal is crucial to resolve MPCs, systems many publications focus on respective systems. For example, the authors of [3] assume ultra-wideband (UWB) signals, while [4–6] target at future cellular signals in the mmWave area.

One approach using bandwidths that are in the range of today's wireless local area network (WLAN) standards is called Channel-SLAM [7, 8]. In Channel-SLAM, the locations and propagation delays of physical and virtual transmitters are estimated jointly with the receiver position in a Rao-Blackwellized particle filter. Since Channel-SLAM does not differentiate between physical and virtual transmitters, it does not differentiate between the LoS component and MPCs either. Each signal component is treated as a signal from a transmitter in a LoS condition.

Hence, maps of estimated transmitter states can be exchanged among users. However, Channel-SLAM is only a relative positioning system, and each user defines their own local coordinate system. When maps are exchanged among users, a map match needs to be performed. We define map matching as (a) estimating the translation and rotation relating the coordinate systems of the user and of a prior map of estimated transmitter states the user receives and (b) finding correspondences among transmitters in that prior map and transmitters observed by the user. In [9], we have presented a map matching scheme that is based on the random sample consensus (RANSAC) [10, 11] framework, and have improved its robustness in [12] by incorporating visibility information [8]. Such visibility information is mapped by the user and describes from which receiver positions the signal from a certain transmitter can be received.

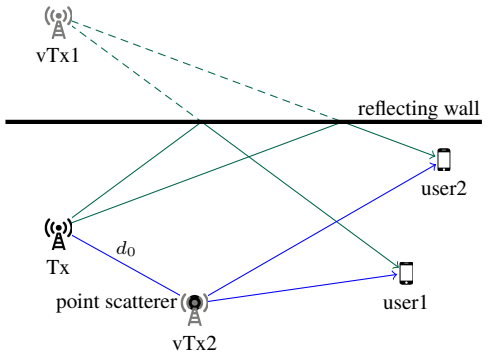

Figure 1: Neglecting the LoS components, the transmit signal from the physical transmitter Tx is received by each user via two different propagation paths. The green MPCs reflected at the wall are regarded as LoS signals from the virtual transmitter vTx1. Similarly, the blue MPCs scattered at the point scatterer are regarded as LoS signals from the virtual transmitter vTx2, which is located at the location of the scatterer.

When a map match has been obtained, i.e., an estimate of the transformation parameters and transmitter correspondences, the information in the prior map can be used for localizing the user equipped with a receiver. An adequate data association scheme to link received signal components with transmitters in the prior map has been presented in [13, 14]. To increase the robustness of data association, visibility information can be used again [15].

Once a user has finished their run in Channel-SLAM, the prior map is updated with observations regarding transmitter states made by the user. Merging the prior map with transmitters observed by the user is denoted by the term map merging [16]. After map merging, the resulting map can be passed on to a next user going through the scenario. Hence, users cooperate by exchanging and improving transmitter maps in a crowd-sourcing like scheme. Turning from a single-user to a cooperative scheme marks a fundamental change in the idea of Channel-SLAM.

In this paper, we present an exhaustive framework for such cooperative Channel-SLAM. We start with an overview of the single-user Channel-SLAM algorithm in Section II. The map matching method based on the RANSAC framework is described in Section III. Section IV presents a map merging scheme. The methods presented in this paper are evaluated by means of simulation data in Section V. Finally, Section VI concludes the paper.

Regarding the notation, $\delta(\cdot)$ is the Dirac delta distribution, and k denotes a time instant. As indices, i identifies a user particle, j a transmitter or a signal component, and ℓ a transmitter particle. In the following, the term user may describe the receiver hardware carried by an actual user depending on the context.

II. MULTIPATH ASSISTED POSITIONING AND SINGLE-USER CHANNEL-SLAM

1. The Principle of Multipath Assisted Positioning

Fig. 1 illustrates the idea of multipath assisted positioning. The LoS signal is neglected for clarity. The transmit signal from the physical transmitter Tx arrives at the two users after traveling along two different propagation paths.

Along the first propagation path drawn in dark green, the signal is reflected in a specular way by the wall representing a planar surface. The resulting MPC is regarded as a LoS signal from the virtual transmitter vTx1, whose location is at the physical transmitter mirrored at the reflecting wall. Since the length of the dark green propagation path and the Euclidean distance between the virtual transmitter vTx1 and the respective user are the same, there is no additional propagation delay between the physical transmitter and the virtual transmitter vTx1. Thus, these two transmitters are perfectly time synchronized.

The second propagation path is drawn in blue. The signal is scattered at the point scatterer. The model of the point scatterer is such that it distributes the energy of the impinging signal uniformly to all directions. The corresponding MPC arriving at the users is regarded as a LoS signal from the virtual transmitter vTx2, which is located at the point scatterer. The length of the blue propagation path involving the point scatterer and the Euclidean distance between the virtual transmitter vTx2 and the respective user are different. This difference is the distance d_0 between the physical and virtual transmitter. Hence, there is an additional propagation delay between the physical transmitter and the virtual transmitter vTx2. This propagation delay can be interpreted as a clock offset.

The above two types of interactions of a signal with an object in the environment, namely reflection at a planar surface and scattering at a point scatterer, can be generalized to multiple interactions in a straightforward manner [8]. In particular, the locations of the virtual transmitters are then still independent from the user positions.

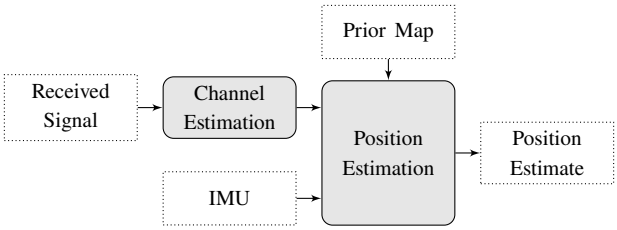

Figure 2: Overview of Channel-SLAM for a single user. In the first stage, a channel estimator estimates and tracks the parameters of signal components. In the second stage, these measurements are used to jointly estimate the user state and the transmitter states.

2. Overview of the Channel-SLAM Algorithm

Channel-SLAM considers a moving user equipped with an antenna array in a static multipath scenario. The physical propagation channel is time-variant due to the movement of the user. It is modeled as a linear superposition of signal components arriving at the user after undergoing different propagation paths. The signal component with index j is described by a time of arrival (ToA) $\tau_j(t)$, which is a synonym for propagation time within the scope of this paper, and a complex amplitude $a_j(t)$. The received signal at the user is expressed at one antenna element at time t as

$$r(\tau, t) = \sum_j a_j(t) s\left(\tau - \tau_j(t)\right) + n(\tau, t), \tag{1}$$

where the random process $n(\tau, t)$ contains both additive white Gaussian noise (AWGN) and dense multipath components (DMCs) [17]. DMCs corresponds to the MPCs which can not be resolved by the measurement aperture.

Channel-SLAM works in two stages as depicted in Fig. 2. In the first stage labeled Channel Estimation, the received signal is sampled and the parameters of the signal components are estimated and tracked over time. In a second step labeled Position Estimation, these estimates are used as measurement inputs in a Bayesian tracking filter, which jointly estimates the position and velocity of the user and the states of the physical and virtual transmitters. Since Channel-SLAM does not differentiate between physical and virtual transmitters, the term transmitter may refer to either one in the following.

In the first stage of Channel-SLAM, snapshots of the received signals are sampled at time instants k. We assume that the channel is constant for the length of one snapshot. Based on these snapshots, the parameters of MPCs are estimated. Depending on the available hardware, such parameters could be ToA, angle of arrival (AoA), or the complex amplitude, for example. Within this paper, we use the Kalman Enhanced Super Resolution Tracking (KEST) estimator [18] for channel estimation, which tracks such parameters over time with Kalman filters. In the inner stage of KEST, namely in the update step of the Kalman filters [19], the Space-Alternating Generalized Expectation-Maximization (SAGE) algorithm [20] is used. The KEST estimator tracks not only the parameters of signal components, but also their current number, which is denoted at time instant k by $N_{\mathrm{TX},k}$. The overall number of transmitters that have been observed by KEST is denoted by $N^{\mathrm{a}}_{\mathrm{TX},k}$. Whenever a new transmitter has been detected, $N^{\mathrm{a}}_{\mathrm{TX},k}$ is increased by one. Tracking the signal components with Kalman filters inherently yields associations among signal components and thus transmitters for neighboring time instants.

As each signal component is regarded as a LoS signal from a transmitter, the KEST estimates are used in the second stage of Channel-SLAM as measurement inputs for the corresponding $N_{\mathrm{TX},k}$ transmitters. Within the scope of this paper, we use the ToA and AoA estimates from KEST. At time instant k, they are stacked in the measurement vector $\boldsymbol{z}_{\mathrm{R},k}$.

The state vector $\boldsymbol{x}_{\mathrm{u},k}$ of the user at time instant k comprises both their two-dimensional position $[x_k \;\; y_k]$ and velocity $[v_{x,k} \;\; v_{y,k}]$, namely

$$\boldsymbol{x}_{\mathrm{u},k} = \left[x_k \;\; y_k \;\; v_{x,k} \;\; v_{y,k}\right]^T. \tag{2}$$

The state vector $\boldsymbol{x}^{<j>}_{\mathrm{TX},k}$ of the j^{th} transmitter at time instant k comprises the location $\left[x^{<j>}_{\mathrm{TX},k} \;\; y^{<j>}_{\mathrm{TX},k}\right]$ and clock offset $\tau^{<j>}_{0,k}$,

$$\boldsymbol{x}^{<j>}_{\mathrm{TX},k} = \left[x^{<j>}_{\mathrm{TX},k} \;\; y^{<j>}_{\mathrm{TX},k} \;\; \tau^{<j>}_{0,k}\right]^T. \tag{3}$$

While the user is assumed to be time synchronized to the physical transmitter, the clock offset covers a possible propagation delay due to scattering of the transmit signal as described in Section II.1.

The joint state vector of the user and the transmitters at time instant k is accordingly given by

$$\boldsymbol{x}^{<j>}_{k} = \left[\boldsymbol{x}_{\mathrm{u},k} \;\; \boldsymbol{x}^{<1>}_{\mathrm{TX},k} \;\; \ldots \;\; \boldsymbol{x}^{<nTXk>}_{\mathrm{TX},k}\right]^T = \left[\boldsymbol{x}_{\mathrm{u},k} \;\; \boldsymbol{x}_{\mathrm{TX},k}\right]^T. \tag{4}$$

In Channel-SLAM, the posterior probability density function (PDF) $\mathrm{p}\left(\boldsymbol{x}_{0:k}|\boldsymbol{z}_{\mathrm{R},1:k},\boldsymbol{u}_{1:k}\right)$ is estimated with recursive Bayesian estimation [19]. The quantities with indices $0{:}k$ and $1{:}k$ refer to the history of the respective quantity from time instants zero to k and one to k, respectively. Measurements $\boldsymbol{u}_{1:k}$ from a gyroscope may be used in the movement model of the user and are denoted by the term control input. With the posterior PDF, the minimum mean square error (MMSE) estimator for the user and the transmitter states is calculated with

$$\hat{\boldsymbol{x}}_{0:k,\mathrm{MMSE}} = \int \boldsymbol{x}_{0:k}\,\mathrm{p}\left(\boldsymbol{x}_{0:k}|\boldsymbol{z}_{\mathrm{R},1:k},\boldsymbol{u}_{1:k}\right)\mathrm{d}\boldsymbol{x}_{0:k}. \tag{5}$$

The posterior PDF can be factorized to

$$\begin{aligned}\mathrm{p}\left(\boldsymbol{x}_{0:k}|\boldsymbol{z}_{\mathrm{R},1:k},\boldsymbol{u}_{1:k}\right) &= \mathrm{p}\left(\boldsymbol{x}_{\mathrm{TX},0:k},\boldsymbol{x}_{\mathrm{u},0:k}|\boldsymbol{z}_{\mathrm{R},1:k},\boldsymbol{u}_{1:k}\right) &(6)\\ &= \mathrm{p}\left(\boldsymbol{x}_{\mathrm{u},0:k}|\boldsymbol{z}_{\mathrm{R},1:k},\boldsymbol{u}_{1:k}\right)\mathrm{p}\left(\boldsymbol{x}_{\mathrm{TX},0:k}|\boldsymbol{x}_{\mathrm{u},0:k},\boldsymbol{z}_{\mathrm{R},1:k}\right), &(7)\\ &= \mathrm{p}\left(\boldsymbol{x}_{\mathrm{u},0:k}|\boldsymbol{z}_{\mathrm{R},1:k},\boldsymbol{u}_{1:k}\right)\prod_{j=1}^{N_{\mathrm{TX},k}}\mathrm{p}\left(\boldsymbol{x}_{\mathrm{TX},0:k}^{<j>}|\boldsymbol{x}_{\mathrm{u},0:k},\boldsymbol{z}_{\mathrm{R},1:k}\right), &(8)\end{aligned}$$

separating the user and the transmitter space in Eq. (7). In Eq. (8), the posterior PDF regarding the transmitter space is factorized into a product of the posterior PDFs regarding the single transmitters [21], and $\boldsymbol{x}_{\mathrm{TX},0:k}^{<j>}$ refers to the history of the state of the j^{th} transmitter.

The implementation of recursive Bayesian estimation is based on a Rao-Blackwellized particle filter [22, 23] as in [8]. The PDFs in a particle filter are represented by weighted samples in the state space, which are called particles. The structure of the Rao-Blackwellized particle filter in Channel-SLAM is such that a user particle filter estimates the user state, i.e., the first factor in Eq. (8). The corresponding posterior PDF regarding the user state history is represented by

$$\mathrm{p}\left(\boldsymbol{x}_{\mathrm{u},0:k}|\boldsymbol{z}_{1:k},\boldsymbol{u}_{1:k}\right) = \sum_{i=1}^{N_p} w_{0:k}^{<i>}\,\delta\left(\boldsymbol{x}_{\mathrm{u},0:k} - \boldsymbol{x}_{\mathrm{u},0:k}^{<i>}\right), \tag{9}$$

where N_p is the number of user particles, $\boldsymbol{x}_{\mathrm{u},0:k}^{<i>}$ the history of the i^{th} user particle and $w_{0:k}^{<i>}$ its associated weight.

For each user particle in the user particle filter, the state of each transmitter is estimated independently from the other user particles and other transmitters. The posterior PDF regarding the j^{th} transmitter and the i^{th} user particle is represented by

$$\mathrm{p}\left(\boldsymbol{x}_{\mathrm{TX},0:k}^{<i,j>}|\boldsymbol{z}_{1:k},\boldsymbol{x}_{\mathrm{u},0:k}^{<i>}\right) = \sum_{\ell=1}^{N_{p,\mathrm{Tx}}} w_{0:k}^{<i,j,\ell>}\,\delta\left(\boldsymbol{x}_{\mathrm{TX},0:k}^{<i,j>} - \boldsymbol{x}_{\mathrm{TX},0:k}^{<i,j,\ell>}\right), \tag{10}$$

where $N_{p,\mathrm{Tx}}$ is the number of transmitter particles, $\boldsymbol{x}_{\mathrm{TX},0:k}^{<i,j,\ell>}$ the history of the ℓ^{th} transmitter particle regarding the j^{th} transmitter and the i^{th} user particle, and $w_{0:k}^{<i,j,\ell>}$ its associated weight. Although the number of transmitter particles $N_{p,\mathrm{Tx}}$ may differ for different time instants, user particles and transmitters, the corresponding indices are omitted in $N_{p,\mathrm{Tx}}$ for notational brevity.

In addition to the states of transmitters, information regarding their visibilities from different locations can be mapped and exploited in Channel-SLAM. Visibility describes whether the transmit signal from a physical or virtual transmitter can be received in a LoS condition and helps detecting loop closures. For example, in Fig. 1, all three transmitters are visible from the two user positions. In [8], we have proposed a scheme where the visibility is mapped in a hexagonal grid map by the user and exploited in the Rao-Blackwellized particle filter for each transmitter. The two-dimensional space is divided into hexagons. For each hexagon and each transmitter, the probability that the transmitter is visible from an arbitrary position within the hexagon is estimated by each user particle. Explicit measurements on which transmitter is visible at time instant k are obtained from the KEST estimator, and they are denoted at time instant k by $\boldsymbol{z}_{\mathrm{V},k}$. The belief that the j^{th} transmitter is visible from the h^{th} hexagon at time instant k is modeled by a Beta distribution [24] with random variable $\boldsymbol{M}_{h,k}^{<j>}$. The corresponding PDF is

$$\mathrm{p}\left(\boldsymbol{M}_{h,k}^{<j>}|\boldsymbol{x}_{\mathrm{u},0:k},\boldsymbol{z}_{\mathrm{V},1:k}\right) = \mathcal{B}\left(\boldsymbol{M}_{h,k}^{<j>};p_{h,k}^{<j>},q_{h,k}^{<j>}\right) = \frac{1}{\mathrm{B}\left(p_{h,k}^{<j>},q_{h,k}^{<j>}\right)}\left(\boldsymbol{M}_{h,k}^{<j>}\right)^{p_{h,k}^{<j>}-1}\left(1-\boldsymbol{M}_{h,k}^{<j>}\right)^{q_{h,k}^{<j>}-1}, \tag{11}$$

omitting the particle index i in $\boldsymbol{M}_{h,k}^{<j>}$ and in the parameters $p_{h,k}^{<j>}$ and $q_{h,k}^{<j>}$ for notational clarity. The function $\mathrm{B}\left(p,q\right)$ is the Beta function for normalization, and the parameters of the Beta distribution are

$$p_{h,k}^{<j>} = C_{h,k}^{<j>} + \nu_h^{<j>} \qquad \text{and} \qquad q_{h,k}^{<j>} = \bar{C}_{h,k}^{<j>} + \bar{\nu}_h^{<j>}. \tag{12}$$

The counters $C_{h,k}^{<j>}$ and $\bar{C}_{h,k}^{<j>}$ count how often the j^{th} transmitter was visible and not visible, respectively, for the user particle in the h^{th} hexagon up to time instant k. The parameters $\nu_h^{<j>}$ and $\bar{\nu}_h^{<j>}$ are used to incorporate prior knowledge and to prevent overly confident conclusions if $C_{h,k}^{<j>}$ and $\bar{C}_{h,k}^{<j>}$ are low.

We define the full measurement vector at time instant k by

$$\boldsymbol{z}_k = \left[\boldsymbol{z}_{\mathrm{R},k}{}^T \;\; \boldsymbol{z}_{\mathrm{V},k}{}^T \right]^T , \tag{13}$$

containing both the radio measurements $\boldsymbol{z}_{\mathrm{R},k}$ and the visibility measurements $\boldsymbol{z}_{\mathrm{V},k}$. Denote the set of the random variables $\boldsymbol{M}_{h,k}^{<j>}$ for all $N_{\mathrm{TX},k}^{\mathrm{a}}$ transmitters and all hexagons the i^{th} user particle has visited up to time instant k by $\boldsymbol{M}_k$. Extending the transmitter state space by visibility information, the posterior PDF regarding the user state and the transmitters' states and visibilities is expressed by

$$\begin{aligned} \mathrm{p}\left(\boldsymbol{x}_{0:k}, \boldsymbol{M}_{0:k} | \boldsymbol{z}_{1:k}, \boldsymbol{u}_{1:k}\right) &= \mathrm{p}\left(\boldsymbol{x}_{\mathrm{TX},0:k}, \boldsymbol{x}_{\mathrm{u},0:k}, \boldsymbol{M}_{0:k} | \boldsymbol{z}_{1:k}, \boldsymbol{u}_{1:k}\right) && (14)\\ &= \mathrm{p}\left(\boldsymbol{x}_{\mathrm{u},0:k}, \boldsymbol{M}_{0:k} | \boldsymbol{z}_{1:k}, \boldsymbol{u}_{1:k}\right) \mathrm{p}\left(\boldsymbol{x}_{\mathrm{TX},0:k} | \boldsymbol{x}_{\mathrm{u},0:k}, \boldsymbol{M}_{0:k}, \boldsymbol{z}_{1:k}, \boldsymbol{u}_{1:k}\right) && (15)\\ &= \mathrm{p}\left(\boldsymbol{x}_{\mathrm{u},0:k}, \boldsymbol{M}_{0:k} | \boldsymbol{z}_{1:k}, \boldsymbol{u}_{1:k}\right) \mathrm{p}\left(\boldsymbol{x}_{\mathrm{TX},0:k} | \boldsymbol{x}_{\mathrm{u},0:k}, \boldsymbol{z}_{1:k}\right) . && (16) \end{aligned}$$

III. EXCHANGING TRANSMITTER MAPS

The methods introduced in the following expand the single-user Channel-SLAM algorithm presented in the previous section by cooperation in exchanging transmitter maps to obtain cooperative Channel-SLAM. When multiple users move through the same scenario, they can exchange maps of estimated transmitter states and visibilities. The transmitter state estimates are represented by the particles and their weights as in Eq. (10), and the visibility information is represented by the parameters in Eq. (12) used in Eq. (11). We denote a set of transmitter state and visibility estimates by the term user map, and a set of estimated transmitter states and visibilities that the user receives by the term prior map. Such a prior map can be provided by a different user, for example [16].

Channel-SLAM is only a relative coordinate system, and each user defines their own local coordinate system. Hence, the transmitter locations are estimated relative to the user location, and the user map and prior map are typically in different coordinate systems that are related by an unknown rotation and translation. Before a user can exploit the information in a prior map, these transformation parameters need to be estimated. This estimation is based on the transmitters in the user map and the prior map. Accordingly, the correspondences among transmitters in the user map and the prior map need to be estimated as well. The joint estimation of the transformation parameters and transmitter correspondences is denoted by the term map matching.

We have presented a scheme for map matching in [9], that is based on the RANSAC algorithm. In RANSAC, a set of parameters of a model is estimated under the presence of so called outliers, i.e., data that are not consistent with the model. Such outliers in map matching are transmitters that are in only one of the two maps and do therefore not have a correspondence in the respective other map. In contrast, inliers are transmitters that do have a correspondence in the respective other map.

An overview of our map matching scheme in the RANSAC framework is presented in Fig. 3. The RANSAC framework is illustrated within the box with black lines. The user map and prior map serve as input. In a first step, three transmitters are chosen randomly from the two maps. This number of transmitters is chosen as it is the minimum number of transmitters necessary to calculate the transformation parameters. In the following steps, it is assumed that the three chosen transmitters from the prior map have correspondences in the three transmitters chosen from the user map.

These correspondences are estimated in the second step of RANSAC based on the relative distances among the transmitters in the two maps [25]. A correspondence set is defined as the set of tuples of the indices of transmitters in the user map and prior map that correspond to each other. These tuples are denoted by $(\mathtt{U}_q, \mathtt{P}_r)$ describing a correspondence between the transmitter with index $\mathtt{U}_q \in \mathcal{U}$ from the user map and a transmitter with index $\mathtt{P}_r \in \mathcal{P}$ from the prior map. The sets $\mathcal{U}$ and $\mathcal{P}$ are the sets of indices of transmitters in the user map and in the prior map, respectively, and are assumed to be distinct for notational convenience. With least squares (LS), we estimate the correspondence set in the s^{th} RANSAC iteration as

$$\hat{\mathcal{C}}_s = \underset{\mathcal{C}_s}{\arg\min} \sum_{(\mathtt{U}_q, \mathtt{P}_r) \in \mathcal{C}_s \wedge (\mathtt{U}_{\tilde{q}}, \mathtt{P}_{\tilde{r}}) \in \mathcal{C}_s} \left(d_{r,\tilde{r}}^{\mathtt{P}} - d_{q,\tilde{q}}^{\mathtt{U}} \right)^2 , \tag{17}$$

where the $\arg\min$ is taken over all possible correspondence sets $\mathcal{C}_s$ of size three. For map matching, only transmitters with a small uncertainty on their state are used from the user and the prior map. Hence, the distance between two transmitters is defined as the Euclidean distance between the means of the two transmitters' state estimates. The distance between two transmitters in the user map with indices $\mathtt{U}_q$ and $\mathtt{U}_{\tilde{q}}$ is denoted by $d_{q,\tilde{q}}^{\mathtt{U}}$. Likewise, the distance of two transmitters in the prior map with indices $\mathtt{P}_r$ and $\mathtt{P}_{\tilde{r}}$ is denoted by $d_{r,\tilde{r}}^{\mathtt{P}}$. Based on the estimated correspondence set in Eq. (17), the transformation parameters are estimated in the third step as in [25]. Again, the estimate obtained with LS.

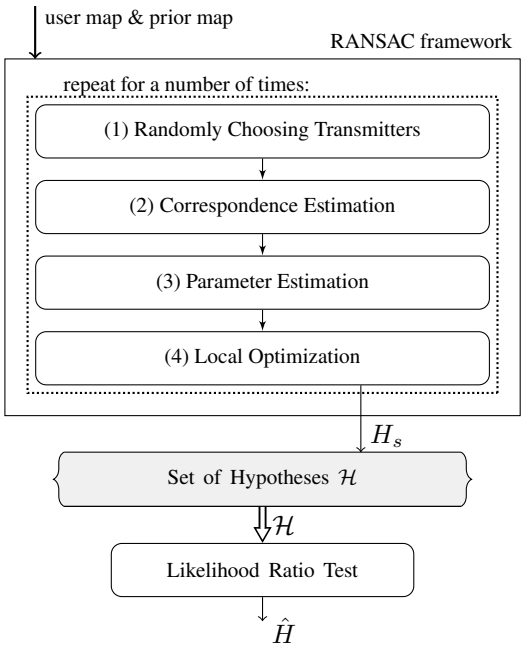

Figure 3: Overview of the map matching scheme. In the RANSAC framework, map matching hypotheses are obtained based on the transmitter states. The subsequent likelihood ratio test is based on transmitter visibilities to resolve possible map matching ambiguities.

The standard RANSAC algorithm assumes that a model estimated with only inliers is consistent with all inliers from the data set. This assumption does not hold in map matching due to possibly biased transmitter state estimates. Therefore, in the fourth step, a local optimization scheme is applied, where the transformation parameters are re-estimated iteratively based on the found transmitter correspondences until convergence is achieved. An additional transmitter correspondence pair is found on a threshold basis, i.e., whenever two transmitters are close enough to each other after the transformation. After the s^{th} iteration, the corresponding hypothesis H_s is added to the set $\mathcal{H}$ of RANSAC hypotheses.

The number of iterations in the RANSAC framework is usually chosen in a probabilistic way. The idea is that with a certain probability, the three transmitters chosen randomly from the prior map do actually correspond to the three transmitters chosen randomly from the user map in at least one iteration. In that case, a valid map matching solution can be found. Each RANSAC iteration results in a hypothesis H_s for a map match, where s is the index of the iteration. The map matching hypotheses are collected in the set $\mathcal{H}$. The final map matching solution $\hat{H}$ is determined by a likelihood ratio test on the hypotheses in $\mathcal{H}$, i.e., the RANSAC solutions from each iteration, and calculated as

$$\hat{H} = \underset{H_s \in \mathcal{H}}{\arg\max}\, \mathrm{p}\left(H_s | \boldsymbol{M}\right) = \underset{H_s \in \mathcal{H}}{\arg\max}\, \mathrm{p}\left(\boldsymbol{M} | H_s\right) \mathrm{p}\left(H_s\right), \tag{18}$$

where $\boldsymbol{M}$ represents the visibility map and hence the test incorporates both the error in the transmitter locations returned by RANSAC in $\mathrm{p}\left(H_s\right)$ and the transmitter visibilities.

To be able to use the prior map after the transformation parameters have been obtained, a reliable data association scheme is necessary. In Channel-SLAM, data association refers to associating signal components with transmitters. In [13, 14], we have presented a multiple hypothesis data association scheme which robustly associates old transmitters and transmitters from a prior map with new signal components detected by the KEST estimator. Old transmitters are transmitters that have been observed by the user at earlier time instants. Data association is important to reduce the high initial uncertainty about the state of transmitters corresponding to newly detected signal components.

Each user particle takes hard decisions for such associations on their own. The ensemble of association decisions taken by the set of user particles can be regarded as a soft decision, though. The set of association decisions by the i^{th} particle at time instant k is denoted by $\mathcal{A}_k^{<i>}$. It contains tuples (a, ν), which describe an association of the new transmitter with index ν and the old or prior map transmitter with index a.

Assume that at time instant k, the KEST estimator detects a new signal component with measurement $\tilde{\boldsymbol{z}}_k^{\text{new}}$ analogue to Eq. (13). The decision by the i^{th} particle at time instant k for associating the newly detected signal component with the old or prior map

transmitter with index a is sampled based on the likelihoods

$$p_a = \mathrm{p}\left(\tilde{\boldsymbol{z}}_{\mathrm{V},k}^{\mathrm{new}} | a, \boldsymbol{M}_{h,k}^{<i>}\right) \sum_{\ell=1}^{N_{p,\mathrm{Tx}}} w_{k-1}^{<i,a_k,\ell>} \, \mathrm{p}\left(\tilde{\boldsymbol{z}}_{\mathrm{R},k}^{\mathrm{new}} | \boldsymbol{x}_{\mathrm{TX},k}^{<i,a_k,\ell>-}, a, \mathcal{A}_{k-1}, \boldsymbol{x}_{\mathrm{u},k}^{<i>}\right), \tag{19}$$

where $\boldsymbol{x}_{\mathrm{TX},k}^{<i,a_k,\ell>-}$ is a transmitter particle after the prediction and before the update in the respective particle filter. The first term on the right hand side of Eq. (19) refers to the visibility of transmitters, while the terms in the sum refer to the transmitter states. The detailed derivation and evaluation of these terms can be found in [8].

Data association for neighboring time instants, i.e., associating signal components from one time step to another, is inherently performed by the Kalman filters in the KEST algorithm as mentioned in Section II.2. With the map matching and data association schemes presented above, prior maps can be incorporated in Channel-SLAM as in Fig. 2 to improve the positioning performance [13].

IV. TRANSMITTER MAP MERGING

With the methods from Section III, a user can use a prior transmitter map that is in a different coordinate system by associating transmitters from the prior map with detected signal components. After the user has finished their movement through the scenario, a *resulting* transmitter map is created by merging the information on the prior map and on the user map, i.e., on observations and measurements by the user. We denote this merging of transmitter information by the term map merging. The resulting map can then be handed over to the next user.

In map merging, we first identify the set of user particles that have not associated the j^{th} of the $N_{\mathrm{TX},k}^{\mathrm{a}}$ transmitters that have been observed by the user up to time instant k with any old or prior map transmitter. The set $\mathcal{T}_j$ contains the indices of these user particles. Since each transmitter can be associated to no more than one other transmitter, $\mathcal{T}_j$ is the set of indices of user particles that could associate the j^{th} transmitter with an old or prior map transmitter.

When a user particle has decided for an association (j, ν), there is an association among the old or prior map transmitter with index j and the new transmitter with index ν. Hence, this particle assumes that the transmitter with index j does not exist, and the respective measurements refer to the transmitter with index ν. Accordingly, the ensemble of user particles has a belief in the existence of each transmitter, which is calculated for the j^{th} transmitter by

$$\mathrm{p}_{e,\mathrm{u}}^{<j>} = \sum_{i \in \mathcal{T}_j} w_k^{<i>}. \tag{20}$$

From map matching, correspondences between transmitters from the prior map and transmitters observed by the user are obtained. For each such correspondence pair, the respective posterior PDFs are merged to obtain the state PDF of the resulting transmitter. PDF are represented in Channel-SLAM by particle clouds. Since a transmitter state PDF tends to converge more and more as the user is in motion and takes measurements from different positions, we merge the transmitters' PDFs based on reliability distances. Assume that we merge the $j_{\mathrm{u}}{}^{\mathrm{th}}$ transmitter observed by the user and the $j_{\mathrm{p}}{}^{\mathrm{th}}$ transmitter from the prior map, i.e., we have an association or correspondence pair $(j_{\mathrm{u}}, j_{\mathrm{p}})$. The reliability distance of the $j_{\mathrm{u}}{}^{\mathrm{th}}$ transmitter observed by the user is defined as

$$\mathrm{d}_{\mathrm{rel,u}}^{<j_{\mathrm{u}}>} = \sum_{i \in \mathcal{T}_{j_{\mathrm{u}}}} w_k^{<i>} \mathrm{d}_{\mathrm{rel,u}}^{<i,j_{\mathrm{u}}>}, \tag{21}$$

where $\mathrm{d}_{\mathrm{rel,u}}^{<i,j_{\mathrm{u}}>}$ denotes the distance the i^{th} user particle has covered while the $j_{\mathrm{u}}{}^{\mathrm{th}}$ transmitter has been visible. Accordingly, each transmitter in the prior map has a reliability distance $\mathrm{d}_{\mathrm{rel,a}}^{<j_{\mathrm{p}}>}$ corresponding to the distances covered by other users while this transmitter was visible. The relative reliability distances of the transmitter with index j that results from merging the user map transmitter with index j_{u} and the prior map transmitter with index j_{p} are defined as

$$\bar{\mathrm{d}}_{\mathrm{rel,u}}^{<j>} = \frac{\mathrm{d}_{\mathrm{rel,u}}^{<j_{\mathrm{u}}>}}{\mathrm{d}_{\mathrm{rel,u}}^{<j_{\mathrm{u}}>} + \mathrm{d}_{\mathrm{rel,a}}^{<j_{\mathrm{p}}>}} \quad \text{and} \quad \bar{\mathrm{d}}_{\mathrm{rel,a}}^{<j>} = \frac{\mathrm{d}_{\mathrm{rel,a}}^{<j_{\mathrm{p}}>}}{\mathrm{d}_{\mathrm{rel,u}}^{<j_{\mathrm{u}}>} + \mathrm{d}_{\mathrm{rel,a}}^{<j_{\mathrm{p}}>}}, \tag{22}$$

respectively.

The particle cloud corresponding to the state PDF of the transmitter with index j resulting from the association $(j_{\mathrm{u}}, j_{\mathrm{p}})$ is defined

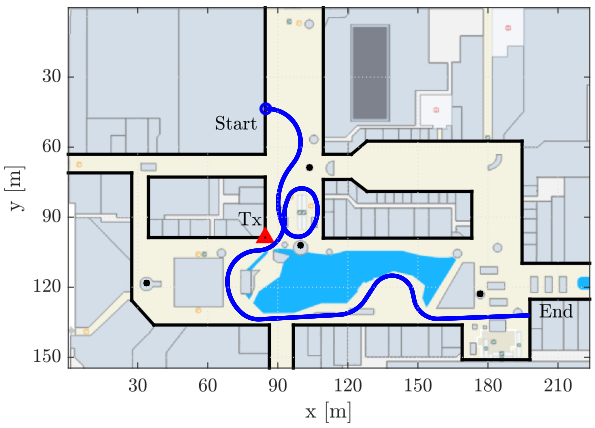

Figure 4: The indoor simulation scenario with one physical transmitter indicated by the red triangle labeled Tx and the reference track depicted by the blue line. Black lines indicate walls that reflect the transmit signal, and black dots represent point scatterers such as pillars.

by

$$\mathrm{p}\left(\boldsymbol{x}_{\mathrm{TX}}^{<j>}\right) = \bar{\mathrm{d}}_{\mathrm{rel,u}}^{<j>} \sum_{\ell=1}^{N_{p,\mathrm{u}}^{<j_\mathrm{u}>}} w_k^{<i,j_\mathrm{u},\ell>} \delta\left(\boldsymbol{x}_{\mathrm{TX}}^{<j>} - \boldsymbol{x}_{\mathrm{TX},k}^{<i,j_\mathrm{u},\ell>}\right) + \bar{\mathrm{d}}_{\mathrm{rel,a}}^{<j>} \sum_{\ell=1}^{N_{p,\mathrm{a}}^{<j_\mathrm{p}>}} w^{<j_\mathrm{p},\ell>} \delta\left(\boldsymbol{x}_{\mathrm{TX}}^{<j>} - \boldsymbol{x}_{\mathrm{TX}}^{<j_\mathrm{p},\ell>}\right), \tag{23}$$

where $\boldsymbol{x}_{\mathrm{TX},k}^{<i,j_\mathrm{u},\ell>}$ is the ℓ^{th} of the $N_{p,\mathrm{u}}^{<j_\mathrm{u}>}$ transmitter particles of the $j_\mathrm{u}{}^{\mathrm{th}}$ transmitter of the i^{th} particle in the user map, $w_k^{<i,j_\mathrm{u},\ell>}$ its associated weight, $\boldsymbol{x}_{\mathrm{TX}}^{<j_\mathrm{p},\ell>}$ the ℓ^{th} of the $N_{p,\mathrm{a}}^{<j_\mathrm{p}>}$ transmitter particles of the $j_\mathrm{p}{}^{\mathrm{th}}$ transmitter in the prior map and $w^{<j_\mathrm{p},\ell>}$ its associated weight.

The number of particles in Eq. (23) is $N_{p,\mathrm{u}}^{<j_\mathrm{u}>} + N_{p,\mathrm{a}}^{<j_\mathrm{p}>}$, and the weights need to be normalized to one. A particle reduction method, for example from [26], can be applied to adapt the number of particles to the uncertainty of the transmitters' state. The lower the uncertainty regarding the transmitter's state, the fewer particles are needed to represent the transmitter.

The reliability distance of the merged transmitter with index j is then defined in a straightforward manner as

$$\mathrm{d}_{\mathrm{rel}}^{<j>} = \mathrm{d}_{\mathrm{rel,a}}^{<j_\mathrm{p}>} + \mathrm{d}_{\mathrm{rel,u}}^{<j_\mathrm{u}>}. \tag{24}$$

The corresponding belief in the existence $\mathrm{p}_e^{<j>}$ is given by

$$\mathrm{p}_e^{<j>} = \mathrm{p}_{e,\mathrm{u}}^{<j_\mathrm{u}>} \bar{\mathrm{d}}_{\mathrm{rel,u}}^{<j>} + \mathrm{p}_{e,\mathrm{a}}^{<j_\mathrm{p}>} \bar{\mathrm{d}}_{\mathrm{rel,a}}^{<j>}, \tag{25}$$

where $\mathrm{p}_{e,\mathrm{u}}^{<j_\mathrm{u}>}$ and $\mathrm{p}_{e,\mathrm{a}}^{<j_\mathrm{p}>}$ are the probabilities of existence of the original transmitters in the user map and in the prior map, respectively. They are obtained from Eq. (20).

Finally, the parameters of the Beta distributions expressing the visibility information regarding the h^{th} hexagon as in Eq. (12) are simply added for the resulting transmitter,

$$p_h^{<j>} = p_{h,k}^{<j_\mathrm{u}>} + p_h^{<j_\mathrm{p}>} \quad \text{and} \quad q_h^{<j>} = q_{h,k}^{<j_\mathrm{u}>} + q_h^{<j_\mathrm{p}>}, \tag{26}$$

where $p_{h,k}^{<j_\mathrm{u}>}$ and $q_{h,k}^{<j_\mathrm{u}>}$ are the parameters of the Beta distributions regarding the $j_\mathrm{u}{}^{\mathrm{th}}$ in the user map, and $p_h^{<j_\mathrm{p}>}$ and $q_h^{<j_\mathrm{p}>}$ the respective parameters of the $j_\mathrm{p}{}^{\mathrm{th}}$ transmitter in the prior map. Since the visibility parameters are essentially counting the number of times a transmitter was visible or not, the reliability distances are inherently employed in these parameters.

V. SIMULATIONS

A top view on the simulation scenario is depicted in Fig. 4. In the scenario, there is one physical transmitter indicated by the red triangle labeled Tx. The thick black lines represent walls that reflect the transmit signal in a specular way, and the black dots represent point scatterers distributing the energy of the impinging electromagnetic wave uniformly to all directions.

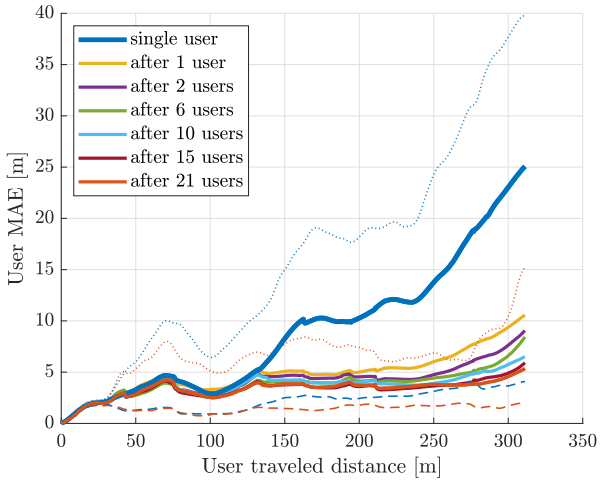

Figure 5: The MAE of the reference user versus their traveled distance. Each curve in a different color corresponds to a number of users that have contributed to a prior map that the reference user has received. For the blue curve labeled single user, the reference user has not received a prior map. The dashed and dotted lines show the 95^{th} and 5^{th} percentiles for the curve in the respective color.

The physical transmitter constantly transmits a signal of $100\,\text{MHz}$ bandwidth with a constant power spectral density. The carrier frequency is at $1.9\,\text{GHz}$. With a rate of $10\,\text{Hz}$, users record snapshots of the received signal and sample it as input for Channel-SLAM.

Each user carries an inertial measurement unit (IMU) with them that is rigidly mounted to the receiver. From the IMU, only turn rates are used as control input in the Rao-Blackwellized particle filter as described in Section II. The antenna arrays of the users consist of nine elements that are arranged in uniform quadratic grid.

For the simulations, the received signal at the user is calculated with ray tracing based on the walls and point scatterers in the scenario. Additionally, white Gaussian noise is added to obtain the received signal.

A user track used for evaluation is depicted in Fig. 4 in blue. We name this track reference track, and a user walking along this track from the point labeled Start to the point labeled End reference user.

Since the location of both the walls and scatterers and the physical transmitter are unknown to the users, the states of the virtual transmitters are as well. The starting position of each user is known to the user in the local coordinate system. However, the users do not know the transformation parameters relating their local coordinate system to the coordinate system in Fig. 4.

For the evaluating the positioning performance, we regard the mean absolute error (MAE) of a user, which is defined at time instant k as

$$\text{MAE}_k = \sum_{i=1}^{N_p} w_k^{<i>} \| \underline{\boldsymbol{p}}_{\text{u},k} - \boldsymbol{p}_{\text{u},k}^{<i>} \|, \tag{27}$$

where $\boldsymbol{p}_{\text{u},k}^{<i>}$ is the position of the i^{th} user particle, $w_k^{<i>}$ the particle's weight, and $\underline{\boldsymbol{p}}_{\text{u},k}$ the true user position.

The positioning error of single-user Channel-SLAM for the reference user is depicted in Fig. 5 by the blue line versus the distance the user has traveled. The positioning error keeps increasing over time, as constantly new transmitters are detected and track of them is lost again. The high uncertainty regarding a transmitter's state upon initialization translates over time in the uncertainty regarding the user position. Only in the region between approximately $70\,\text{m}$ and $100\,\text{m}$, the MAE decreases, as the user goes in a loop and the data association scheme can associate previously observed with newly detected transmitters. In particular near the end of the track, the geometrical dilution of precision (GDoP) further decreases the positioning performance, since all of the dominant signal components arrive at the user from a similar direction.

In addition to the MAE, the 95^{th} and 5^{th} percentiles are plotted with a dashed and a dotted blue line, respectively. Thus, in $95\,\%$ of the simulation runs, the MAE was below the dashed blue line, and in $5\,\%$, it was below the dotted blue line.

For evaluating cooperative Channel-SLAM, we consider 21 users going along the tracks depicted in Fig. 6, showing the same scenario as Fig. 4. The starting points of each track is marked by a circle. The first of the 21 users has no prior information on transmitter states in form of a prior map and walks through the scenario with single-user Channel-SLAM. The transmitter map that this first user creates is then successively passed on to the respective next user. Each of the next users walks along their track, performs map matching to transform the map into their own coordinate system, uses the information about transmitter estimates

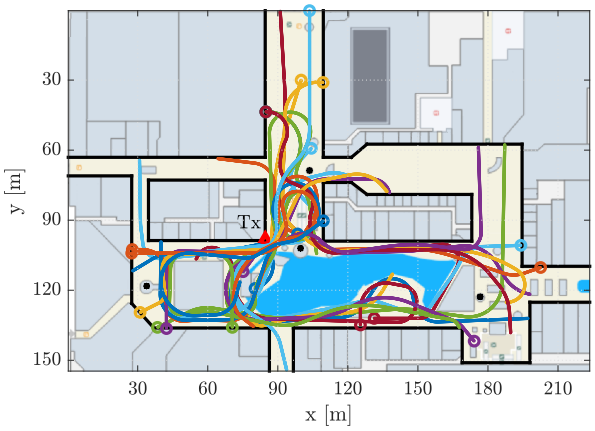

Figure 6: The simulation scenario with the 21 user tracks used for creating a prior transmitter map. The start point of each track is indicated by a circle.

in the map, improves it with own observations in map merging and passes it on to the next user. Hence, each time the map is passed on to the next user, it becomes better and more complete in terms of transmitter state and visibility estimates.

The reference user now walks along their track with a prior transmitter map to which a number of the 21 users have contributed. The more users have contributed to the transmitter map, the better becomes the positioning performance of the reference user. In Fig. 5, the MAE is plotted for the reference user after one, two, six, 15 and finally all 21 users have contributed to the map. For the last case, the 95^{th} and 5^{th} percentiles are plotted as well with a dashed and a dotted red line, respectively. We can observe that even after few users have contributed to the map, the positioning performance of the user improves considerably. The more user have contributed, the better the positioning performance, especially near the end of the reference user track with an unfavorable GDoP.

VI. CONCLUSION

This paper has presented a comprehensive overview on the framework of cooperative Channel-SLAM. The transformation parameters relating the coordinate systems of different users are estimated with map matching when maps of transmitters are exchanged. Map matching and map merging turn Channel-SLAM from a single-user to a cooperative multipath assisted positioning system. We have shown how visibility information is incorporated in both matching and map merging.

Our evaluations show that the positioning performance of Channel-SLAM is increased considerably compared to the single-user case. In the long run, the positioning error for non-cooperative users keeps increasing over time. In contrast, the positioning performance is bounded for cooperative users in the same scenario at around 5 m for a signal bandwidth of only 100 MHz.

ACKNOWLEDGEMENT

This work was partially supported by the DLR project Navigation 4.0.

REFERENCES

[1] H. Durrant-Whyte and T. Bailey, “Simultaneous Localization and Mapping: Part I,” *IEEE Robot. Autom. Mag.*, vol. 13, no. 2, pp. 99–110, Jun. 2006.

[2] T. Bailey and H. Durrant-Whyte, “Simultaneous Localization and Mapping (SLAM): Part II,” *IEEE Robot. Autom. Mag.*, vol. 13, no. 3, pp. 108–117, Sep. 2006.

[3] E. Leitinger, F. Meyer, F. Tufvesson, and K. Witrisal, “Factor Graph Based Simultaneous Localization and Mapping Using Multipath Channel Information,” in *IEEE International Conference on Communications Workshops (ICC Workshops 2017)*, May 2017, pp. 652–658.

[4] K. Witrisal, P. Meissner, E. Leitinger, Y. Shen, C. Gustafson, F. Tufvesson, K. Haneda, D. Dardari, A. F. Molisch, A. Conti, and M. Z. Win, “High-Accuracy Localization for Assisted Living - 5G Systems will turn Multipath Channels from Foe to Friend,” *IEEE Signal Process. Mag.*, vol. 33, no. 2, pp. 59–70, Mar. 2016.

[5] A. Shahmansoori, G. E. Garcia, G. Destino, G. Seco-Granados, and H. Wymeersch, "Position and Orientation Estimation Through Millimeter-Wave MIMO in 5G Systems," *IEEE Trans. Wireless Commun.*, vol. 17, no. 3, pp. 1822–1835, 2018.

[6] R. Mendrzik, H. Wymeersch, G. Bauch, and Z. Abu-Shaban, "Harnessing NLOS Components for Position and Orientation Estimation in 5G Millimeter Wave MIMO," *IEEE Trans. Wireless Commun.*, vol. 18, no. 1, pp. 93–107, Jan. 2019.

[7] C. Gentner, T. Jost, W. Wang, S. Zhang, A. Dammann, and U.-C. Fiebig, "Multipath Assisted Positioning with Simultaneous Localization and Mapping," *IEEE Trans. Wireless Commun.*, vol. 15, no. 9, pp. 6104–6117, Sep. 2016.

[8] M. Ulmschneider, S. Zhang, C. Gentner, and A. Dammann, "Multipath Assisted Positioning With Transmitter Visibility Information," *IEEE Access*, vol. 8, pp. 155 210–155 223, 2020.

[9] M. Ulmschneider and C. Gentner, "RANSAC for Exchanging Maps in Multipath Assisted Positioning," in *IEEE International Conference on Industrial Cyber Physical Systems (ICPS)*, 2019.

[10] M. A. Fischler and R. C. Bolles, "Random Sample Consensus: A Paradigm for Model Fitting with Applications to Image Analysis and Automated Cartography," *Commun. ACM*, vol. 24, no. 6, pp. 381–395, Jun. 1981.

[11] R. Raguram, J.-M. Frahm, and M. Pollefeys, "A Comparative Analysis of RANSAC Techniques Leading to Adaptive Real-Time Random Sample Consensus," in *Computer Vision – ECCV 2008*, 2008, pp. 500–513.

[12] M. Ulmschneider, C. Gentner, and A. Dammann, "Matching Maps of Physical and Virtual Radio Transmitters Using Visibility Regions," in *Proceedings of IEEE/ION PLANS 2020*, May 2020.

[13] M. Ulmschneider, C. Gentner, T. Jost, and A. Dammann, "Association of Transmitters in Multipath-Assisted Positioning," in *IEEE Global Communications Conference (GLOBECOM)*, Dec. 2017.

[14] ——, "Multiple Hypothesis Data Association for Multipath-Assisted Positioning," in *14th Workshop on Positioning, Navigation and Communications (WPNC)*, Oct. 2017.

[15] M. Ulmschneider, C. Gentner, and A. Dammann, "Data Association among Physical and Virtual Radio Transmitters with Visibility Regions," in *IEEE 90th Vehicular Technology Conference (VTC2019-Fall)*, Sep. 2019.

[16] M. Ulmschneider and C. Gentner, "Improving Maps of Physical and Virtual Radio Transmitters," in *Proceedings of the 31st International Technical Meeting of the Satellite Division of The Institute of Navigation (ION GNSS+ 2018)*, Sep. 2018.

[17] A. Richter, "Estimation of Radio Channel Parameters: Models and Algorithms," Ph.D. dissertation, Technische Universität Ilmenau, 2005.

[18] T. Jost, W. Wang, U. Fiebig, and F. Perez-Fontan, "Detection and Tracking of Mobile Propagation Channel Paths," *IEEE Trans. Antennas Propag.*, vol. 60, no. 10, pp. 4875–4883, Oct. 2012.

[19] S. Kay, *Fundamentals of Statistical Signal Processing: Estimation Theory*, ser. Fundamentals of Statistical Signal Processing. Prentice-Hall PTR, 1998.

[20] B. Fleury, M. Tschudin, R. Heddergott, D. Dahlhaus, and K. Pedersen, "Channel Parameter Estimation in Mobile Radio Environments Using the SAGE Algorithm," *IEEE J. Sel. Areas Commun.*, vol. 17, no. 3, pp. 434–450, Mar. 1999.

[21] S. Thrun, M. Montemerlo, D. Koller, B. Wegbreit, J. Nieto, and E. Nebot, "FastSLAM: An Efficient Solution to the Simultaneous Localization And Mapping Problem with Unknown Data Association," *Journal of Machine Learning Research*, vol. 4, no. 3, pp. 380–407, 2004.

[22] M. Arulampalam, S. Maskell, N. Gordon, and T. Clapp, "A Tutorial on Particle Filters for Online Nonlinear/non-Gaussian Bayesian Tracking," *IEEE Trans. Signal Process.*, vol. 50, no. 2, pp. 174–188, Feb. 2002.

[23] A. Doucet, S. Godsill, and C. Andrieu, "On Sequential Monte Carlo Sampling Methods for Bayesian Filtering," *Statistics and Computing*, vol. 10, no. 3, pp. 197–208, Jul. 2000.

[24] G. Andrews, R. Askey, and R. Roy, *Special Functions*, ser. Encyclopedia of Mathematics and its Applications. Cambridge University Press, 1999.

[25] M. Ulmschneider, D. C. Luz, and C. Gentner, "Exchanging Transmitter Maps in Multipath Assisted Positioning," in *Proceedings of IEEE/ION PLANS 2018*, May, 2018.

[26] C. Gentner, R. Pöhlmann, M. Ulmschneider, T. Jost, and S. Zhang, "Positioning Using Terrestrial Multipath Signals and Inertial Sensors," *Mobile Information Systems*, 2017.